Environmental Science Nano

PAPER

View Article Online
View Journal

Cite this: DOI: 10.1039/d4en00063c

Capping drives the behavior, dissolution and (eco) toxicity of silver nanoparticles towards microorganisms and mammalian cells†

Arianna Bellingeri, *[ab] Nina Bono, *[c] Iole Venditti, [d] Federica Bertelà,[d] Luca Burratti,[d] Claudia Faleri,[e] Giuseppe Protano,[a] Eugenio Paccagnini,[e] Pietro Lupetti,[e] Gabriele Candiani [c] and Ilaria Corsi [ab]

Received 23rd January 2024,
Accepted 9th March 2024

DOI: 10.1039/d4en00063c

rsc.li/es-nano

Surface coating plays a fundamental role in driving silver nanoparticle (AgNP) toxicity towards cells, but no clarity exists on the mechanism behind it. AgNPs with two different capping agents, citrate and L-cysteine (citLcys) and sodium-3-mercapto-1-propanesulfonate (3MPS), developed as sensors for metal ions in water (*e.g.*, Hg(II) and Ni(II)), were investigated in terms of (eco)toxicity towards bacteria (*Escherichia coli*), microalgae (*Raphidocelis subcapitata* and *Phaeodactylum tricornutum*) and mammalian cells (HeLa and L929). After 72 h of incubation, Ag ion dissolution in algal media was negligible (<1% of nominal AgNP concentration) for both batches. Suspension in protein-rich media showed the formation of a protein corona around AgNPcitLcys as opposed to AgNP3MPS, which was confirmed by dynamic light scattering (DLS) analysis, transmission electron microscopy (TEM) and one-dimensional polyacrylamide gel electrophoresis (1D-PAGE). Low toxicity was observed for both AgNPs towards microalgae (≥5 mg L^{-1}) and *E. coli* (≥256 mg L^{-1}) and no effect was observed on HeLa and L929 cells. However, the responses suggest that citLcys coating might trigger the onset of a nano-size related toxicity as opposed to 3MPS, whose toxicity mainly relies on dissolution. Our findings show how surface coating rules AgNP interaction with biomolecules and drives AgNP (eco)toxicity towards cells, thus influencing exposure outcome.

Environmental significance

Surface capping strongly conditions nanosilver behavior in media with different compositions. Given the wide variety of conditions encountered by silver nanoparticles in experimental settings, the mechanisms involved in the onset of toxicity are easily misread. The comparison of differently capped silver nanoparticles on cells and unicellular microorganisms, each living and growing in a different environment, gives useful insights into the understanding of the role played by surface capping in defining nanosilver (eco)toxicity. The design of adequate capping can significantly reduce the risks to humans and the environment while maintaining unaltered properties of the nanomaterial itself. More attention should be spent on thinking nanosilver capping in order to meet safety and sustainability by design requirements for safer next-generation nanomaterials.

1. Introduction

Over the last decades, nanomaterials are at the leading edge of the rapidly developing field of nanotechnology. Their unique size-dependent properties make these materials irreplaceable in many areas, including catalysis, imaging, medical applications, energy-based research, and environmental applications as nanoremediation.[1–3]

In this framework, nanotechnology-based solutions, in particular silver nanoparticles (AgNPs or nanosilver), have recently emerged as promising candidates. AgNPs are easily synthesized and functionalized, cost-effective, and display enhanced broad-range antimicrobial properties against bacteria, fungi, and viruses.[4] Furthermore, more functionalities that induce specific properties have recently

[a] *Department of Physical, Earth and Environmental Sciences, University of Siena, Via Mattioli 4, 53100 Siena, Italy. E-mail: arianna.bellingeri2@unisi.it, giuseppe.protano@unisi.it, ilaria.corsi@unisi.it; Tel: +39 0577 232811*
[b] *NBFC, National Biodiversity Future Center, Palermo 90133, Italy*
[c] *Department of Chemistry, Materials and Chemical Engineering "Giulio Natta", Politecnico di Milano, Via Mancinelli 7, 20131, Milano, Italy. E-mail: nina.bono@polimi.it, gabriele.candiani@polimi.it*
[d] *Department of Sciences, Roma Tre University of Rome, Via della Vasca Navale 79, 00146 Rome, Italy. E-mail: iole.venditti@uniroma3.it, federica.bertelà@uniroma3.it, luca.burratti@uniroma3.it*
[e] *Department of Life Sciences, University of Siena, Via Aldo Moro 2, 53100, Siena, Italy. E-mail: claudia.faleri2@unisi.it*

† Electronic supplementary information (ESI) available. See DOI: https://doi.org/10.1039/d4en00063c

been introduced onto AgNP surface; this can be exploited in the field of environmental protection to induce hydrophilic features and selective interaction with water pollutants and/or antibacterial activity.[5–8]

However, the massive production and use of nano-enabled products containing AgNPs have caused their release in sewage waters and, consequently, in the resulting sludge and treated waters,[9] with predicted environmental concentrations (PECs) for surface waters in the range of μg L^{-1}.[10,11] Many strains of microalgae and bacteria have been shown to be affected by AgNP exposure[12–16] with effective concentrations ranging from μg L^{-1} to mg L^{-1}. Microorganisms are the basic constituents of aquatic food webs and play a central role in ecosystem regulation and balance.[17] Shifts in microbial communities upon exposure to AgNPs have been recently documented with potential effects on nutrient cycle processes, for example by inhibiting nitrification.[17]

It is well known that the toxicity of AgNPs is closely related to the dissolution and subsequent release of Ag ions (Ag^+).[12,18,19] Besides, direct physical interactions between AgNPs and the surface/membrane of microorganism also give rise to some toxic effects.[18,20] Such interactions closely depend on the target microorganism, the time of exposure, as well as the binding strength between AgNPs and the organism's surface/membrane. This, in turn, relies on AgNP features, such as size, shape, surface coating and charge, as well as any other transformation occurring upon AgNP suspension in aqueous media, whose properties affect NP behaviour and fate (*e.g.*, salinity and organic molecules such as proteins and sugars).[21–23]

In particular, the surface properties of AgNPs have a crucial role as they influence both physical (aggregation, affinity for biomolecules, *etc.*) and chemical (dissolution, reactivity, *etc.*) transformations. Although several impairments of cellular functions have been reported upon the exposure to AgNPs, the majority of studies often lack in providing detailed information about NP behaviour and modification in exposure media, which are key elements in understanding nano–bio-interactions, mode of action (MoA) and apical (eco)toxicity.

Herein, we seek to shed more light on the role of AgNP coatings on the (eco)toxicity towards unicellular microorganisms and mammalian cells. To this aim, two types of AgNPs, one functionalized with citrate and L-cysteine (AgNPcitLcys) and the other one with sodium-3-mercapto-1-propanesulfonate (AgNP3MPS), both developed as sensors for metal ions (*i.e.*, mercury and nickel) in water media, were fully characterized in different exposure media and tested.[24–27] Unicellular microorganisms, such as Gram-negative bacteria *Escherichia coli*, freshwater microalgae *Raphidocelis subcapitata* and marine microalgae *Phaeodactylum tricornutum* and mammalian cells (HeLa, L929), were selected for investigating the mechanism of (eco) toxicity along with transformation occurring in exposure media and bio–nano-interactions.

2. Materials and methods

2.1. Materials

Reagents and solvents of analytical grade were purchased from Sigma-Aldrich (St. Louis, MO) and used without further purification: silver nitrate ($AgNO_3$, 99.9% pure), sodium citrate ($Na_3C_6H_5O_7$, citr, 99% pure), L-cysteine ($C_3H_7NO_2S$, 97% pure), 3-mercapto-1-propanesulfonic acid sodium salt ($C_3H_7S_2O_3Na$, 98% pure) and sodium borohydride ($NaBH_4$, 99.9% pure).

E. coli JM 109 (Gram-negative bacterial strain, biosafety level 1) was purchased from Leibniz Institute DSMZ – German Collection of Microorganisms and Cell Cultures (Braunschweig, Germany). HeLa (human cervix carcinoma, ATCC®-CCL-2) and L929 (murine fibroblast from subcutaneous connective tissue; ATCC®-CCL-1TM) cell lines were purchased from the American Type Culture Collection (ATCC, Manassas, VA, USA). LB broth (cod. no. L3022) and Dulbecco's modified Eagle's medium (DMEM) were from Merck Life Science S.r.l. (Milan, Italy). AlamarBlue Cell Viability Assay® was purchased from Life Technologies Italia (Monza, Italy).

R. subcapitata (freshwater microalga) was obtained from the Italian Institute for Environmental Protection and Research (ISPRA) and cultured in TG201 medium (Table S1†). *P. tricornutum* (marine microalga) was obtained from the Regional Agency for Environmental Protection of Tuscany (ARPAT) and cultured in F/2 medium, (Table S1†).

2.2. AgNP synthesis

AgNPcitLcys were synthesized according to Prosposito *et al.*[24] and Bertelà *et al.*[26] Briefly, 10 mL of citrate solution (0.01 M in deionized water (dH_2O)), 25 mL of L-cysteine solution (0.002 M in dH_2O) and 2.5 mL of silver nitrate ($AgNO_3$) solution (0.05 M in dH_2O) were sequentially added in a 100 mL flask under stirring. The mixture was degassed with argon for 10 min, then 4 mL of sodium borohydride ($NaBH_4$) solution (0.016 g in 4 mL of dH_2O) were added. The mixture was allowed to react at room temperature (r.t.) for 2 h, and then the brown solution was collected.

AgNP3MPS were synthesized with slight changes from the previous literature.[27,28] Briefly, $NaBH_4$ (0.0151 g in 100 mL of dH_2O, solution A) was cooled to 3 °C under vigorous stirring. A 10 mL aliquot was withdrawn from solution A and used to dissolve 0.2 g of 3MPS (solution B). The solution of $AgNO_3$ (solution C) was prepared at a concentration of 2 mM (0.0342 g in 100 mL of dH_2O). A volume of 6 ml of solution C was added into solution A at approximately one drop per second. A volume of 11 μL of solution B was injected and the magnetic stirring was suddenly stopped. Solutions were centrifuged at 13 000 rpm for 20 min (twice) and resuspended in dH_2O. The obtained AgNPcitLcys and AgNP3MPS were stored at 4 °C until use.

2.3. AgNP characterization

2.3.1. Physico-chemical characterization of AgNPs. AgNPs (100 mg L^{-1}) were suspended in Milli-Q water, microalgae culture media (TG201 for *R. subcapitata* and F/2 for *P. tricornutum*), *E. coli* growth medium (LB), and HeLa L929 culture medium (cDMEM) (for media composition, please refer to Table S1†). The hydrodynamic diameter (D_H, nm), polydispersity index (PDI), and ζ-potential (ζ_P, mV) of AgNPcitLcys and AgNP3MPS suspensions were measured by Dynamic Light Scattering (DLS) and laser Doppler micro-electrophoresis using a Zetasizer Nano (ZS90, Malvern, Italy), fitted with a 5 mW HeNe laser (λ = 633 nm) and a scattering angle of 173°. Measurements were run in triplicate and carried out at 25 °C.

2.3.2. Structural characterization of AgNPs. Transmission Electron Microscopy (TEM) of the same AgNPcitLcys and AgNP3MPS suspensions (Milli-Q water, TG201, F/2, cDMEM and LB medium) was also performed. For protein-free media (Milli-Q water, TG201 and F/2), images were obtained with a Philips Morgagni 268 D electronics at 80 KV, equipped with a MegaView II CCD camera, at 10 mg L^{-1} of AgNPcitLcys and 50 mg L^{-1} of AgNP3MPS, respectively, the latter to capture smaller sizes.

The formation of a protein corona upon incubation with protein-rich media (LB and cDMEM) was inspected by incubating AgNPs at 37 °C for 120 min in 2 mL of LB or cDMEM (final concentration: 0.5 g AgNPs L^{-1}). Samples were then centrifuged at $1.6 \times 10^4 g$ for 20 min, and pellets were washed 3 times with PBS. Samples were resuspended in 1 mL PBS and investigated by TEM (Tecnai G2 Spirit (FEI)).

2.3.3. Ag ion release. Ag ion (Ag^+) release from AgNPcitLcys and AgNP3MPS was determined in TG201 and F/2 suspensions at 60 mg L^{-1} and in LB broth at 256 mg L^{-1}. For Ag^+ release tests in microalgae culture media, AgNPs were kept at 21 °C and continuous illumination (4500 lux) for 72 h; when in LB broth, AgNPs were kept at 37 °C in the dark for 24 h. In both conditions, AgNP suspensions were mixed by manual shaking once a day. From each suspension, an aliquot was taken at two different time points (*i.e.*, 1 h and 24 or 72 h post incubation) and centrifuged (5000*g* for 40 min) using a 3 kDa cut-off filter device (Amicon Ultra-15 mL, Millipore, USA). Eluates were further processed for Ag quantification by inductively coupled plasma-mass spectrometry (ICP-MS) using the PerkinElmer NexION 350 spectrometer (Waltham, MA, USA). Ag was also measured in media (TG201, F/2, and LB) and media supplemented with $AgNO_3$ (7 μg L^{-1}). The analytical accuracy was checked by comparing the certified and measured Ag concentration in the standard reference material SRM 1643e (Institute of Standards and Technology, NIST), while the analytical precision was evaluated through the percentage relative standard deviation (% RSD) of five replicate analyses of each water sample.

2.3.4. Protein corona isolation and one-dimensional polyacrylamide gel electrophoresis (1D-PAGE). To investigate the formation of protein corona in exposed media, AgNPcitLcys and AgNP3MPS were incubated at 37 °C for 120 min in 2 mL of LB or cDMEM (final concentration: 0.5 g AgNPs L^{-1}). Next, samples were centrifuged at $1.6 \times 10^4 g$ for 20 min, then pellets were washed 3 times with PBS. LB and cDMEM were run in parallel to rule out eventual protein pelleting in the absence of AgNPs. Supernatants were discarded and the pellets solubilized in 60 μL of extraction buffer (50 mM HEPES pH 7.4, 1 mM PMSF, 2 μg mL^{-1} leupeptin, 2 μg mL^{-1} aprotinin, 1 μg mL^{-1} pepstatin, 1% (v/v) Triton X-100).[29]

For 1D-PAGE, proteins were diluted in Laemmli buffer and boiled for 5 min, loaded in a 4–15% Mini-PROTEAN® TGX™ Gel precast polyacrylamide gel (Bio-Rad Laboratories), and run for ≈60 min at 130 V. Next, gels were washed in dH_2O (3 times), then stained with Bio-Safe Coomassie Stain, and imaged using a Gel Doc™ EZ System and Image Lab Software 4.0 (Bio-Rad Laboratories).

2.4. (Eco)toxicity assessment

2.4.1. Bacteria. The *in vitro* antibacterial activity of AgNPcitLcys and AgNP3MPS against rapidly growing aerobic bacteria was assessed according to the EN ISO 20776-1:2020 norm.[30]

E. coli bacteria were pre-cultured overnight at 37 °C in 5 mL of LB broth under shaking at 130 rpm, until reaching an optical density (OD_{600nm}) of ≈1, corresponding to ≈10^9 bacteria per mL. The bacterial suspension was next diluted to a concentration of ≈10^6 bacteria per mL and 50 μL mixed with 50 μL of AgNPcitLcys and AgNP3MPS suspensions at various concentrations into separate wells of a 96-multiwell plate (n = 3 wells/concentration/AgNP type) at 37 °C for 24 h. AgNPcitLcys and AgNP3MPS suspensions at final concentrations ranging from 0.06 to 250 mg L^{-1} (2-fold serial dilution) were used to assess the antibacterial activity. Bacteria inoculated in 50 μL of LB were used as negative controls of bacterial growth ($^-$CTRL, n = 3), while bacteria inoculated with $AgNO_3$ at different concentrations were used as the positive control ($^+$CTRL).

The antibacterial efficacy was evaluated after 24 h incubation by means of the turbidity method (*i.e.*, OD_{600nm} measurements)[31,32] using a GENios Plus spectrophotometer (Tecan, Milan, Italy). For each AgNP concentration, the antibacterial efficiency was calculated as follows.

$$\text{Antibacterial activity (\%)} = (1 - (OD_{600nm,sample}/OD_{600nm,CTRL})) \times 100.$$

2.4.2. Microalgae. Algal toxicity tests were performed using the freshwater microalga *R. subcapitata* and the marine microalga *P. tricornutum* following standardized protocols OECD 201 2011.[33,34] Microalgae were cultured in TG201 medium (*R. subcapitata*), prepared using Milli-Q water as the dilution water, and F/2 medium (*P. tricornutum*), prepared using filtered (0.45 μm) natural seawater (NSW) as the

dilution water and maintained in axenic exponential growth conditions at 18 ± 1 °C with a 16/8 h light–dark cycle photoperiod in a growth chamber.

Toxicity tests (72 h) were carried out in modified growth media to limit the amount of chelating agents (*i.e.*, EDTA), following recommendations for heavy metal toxicity testing.[35,36] The final EDTA concentration in test media was 50 μg L^{-1} in TG201 and 800 μg L^{-1} in F/2, which were previously optimized to ensure the optimal growth of both algae.

Algae were pre-cultured for 72 h before running the assay and maintained at 21 ± 1 °C and continuous illumination at 4500 lux. Tests were carried out in 24-multi-well plates with a 2 mL capacity for each well. Initial algal concentration in toxicity tests was 1 × 10^4 cells per mL and exposure concentrations of AgNPcitLcys and AgNP3MPS were 0, 1, 5, 10, 15, 30, and 60 mg L^{-1}, while for $AgNO_3$, different concentrations were chosen based on species-specific sensitivity: 0, 1, 3, 5, 7, 10, and 100 μg L^{-1} for *R. subcapitata* and 0, 1, 5, 10, 50, 100, 500, and 1000 μg L^{-1} for *P. tricornutum*. $AgNO_3$ was used as a positive control. Three replicates for each exposure concentration were set. *R. subcapitata* multi-well plates were placed over an orbital shaker at 50 rpm to reduce algal settling and enable gas exchanges. Every test was repeated three times. After 72 h, algae were fixed with a 1 : 1 (v/v) Lugol/ethanol solution, and cell number was estimated both by counting under an optical microscope (Olympus BX51, 40×) equipped with an improved Neubauer chamber and utilizing an automated cell counter (LUNA II, Logos Biosystems) for *R. subcapitata*. Microalgae concentration (cells mL^{-1}), growth rate (μ), and growth inhibition (Iμi) compared to the control were determined.

2.4.3. Mammalian cells. To assess the *in vitro* cytotoxicity of AgNPs to HeLa and L929 cell lines, indirect cytotoxicity tests were performed according to the ISO 10993-5 standard norm.[37]

Briefly, mycoplasma-free HeLa and L929 cell lines were cultured in cDMEM in a humidified atmosphere under a constant supply of 5% CO_2 and at 37 °C (hereinafter referred to as standard culture conditions).

Cells were seeded in 96-multiwell plates at a density of 10^4 cells per well in 100 μL of cDMEM and incubated in standard culture conditions for 24 h. Afterward, the medium of each well was replaced with 100 μL per well of AgNPcitLcys-, AgNP3MPS- or $AgNO_3$-containing medium (AgNP concentrations ranging from 0.06 mg L^{-1} to 250 mg L^{-1}) and further incubated for 24 h in standard culture conditions. Cells cultured in cDMEM were used as negative controls of cytotoxicity ($CTRL^-$), while cells cultured in $AgNO_3$ and 0.5% phenol solution in cDMEM served as positive controls of cytotoxicity ($CTRL^+$). Tests were performed in triplicate.

Following 24 h-incubation, the cell viability was assessed using AlamarBlue cell viability assay (Life Technologies Italia, Monza, Italy). Briefly, the medium was replaced with 100 μL of cDMEM containing 10 μL of 10× resazurin dye solution. Cells were incubated in standard culture conditions for 2 h and the fluorescence of the medium was read using a Synergy H1 spectrophotometer (BioTek, Italy) (λ_{ex} = 540 nm; λ_{em} = 595 nm). The viability of $CTRL^-$ was assigned as 100%, and the cytotoxicity was calculated according to the following equation

$$\begin{aligned}\text{Cytotoxicity (\%)} &= 100\% - \text{Viability (\%)} \\ &= (1 - (F_{AgNPs}/F_{CTRL^-})) \times 100\end{aligned}$$

where F is the recorded fluorescence.

2.5. Statistical analyses

Statistical analyses were carried out with GraphPad version 8 (GraphPad Software, La Jolla, CA, USA). EC_{50} values were calculated using non-linear regression analysis, while statistical significance between mean values was calculated with a non-parametric test (Kruskal–Wallis test). Significance was retained when $p < 0.05$. Data are expressed as mean ± standard deviation (SD). Experiments were performed at least in triplicate.

3. Results and discussion

3.1. AgNPs behavior and interaction with media components

As shown by DLS data (Table 1), in Milli-Q water AgNP3MPS showed an average small nominal size (D_H = 2 ± 1 nm) while AgNPcitLcys are one order of magnitude larger (D_H = 12.5 ± 1 nm) (Table 1 and Fig. S1†), also confirmed by TEM images (Fig. 1a and b). Both AgNPcitLcys and AgNP3MPS resulted negatively charged with a ζ_P of ≈ −42 mV and ∼−33 mV (Table 1) in agreement with our previous findings.[24,38]

The physicochemical features of AgNPs were strongly affected by the chemical composition of the suspension media. In this study, we employed media largely differing in salinity (TG201 < F/2), osmolality (TG201 < LB < cDMEM < F/2) and conductivity (TG201 < LB < cDMEM < F/2) (Table S2†), which indeed played a role in influencing the AgNPs behaviour. AgNPcitLcys D_H were found to be linearly influenced by salinity in TG201 and F/2, increasing the aggregation along with ionic strength (Table 1). ζ_P values confirm such observations as they approach neutrality with increasing salinity. In LB and cDMEM media, both D_H and ζ-potential values fall in between those obtained for algal media, highlighting the influence of the increased osmolality and conductivity on AgNPcitLcys behaviour.

AgNP3MPS behaviour differs from that of AgNPcitLcys. In fact, while the different salinity of TG201 and F/2 still affect aggregation and stability, the higher osmolality and conductivity of LB and cDMEM do not seem to translate into enhanced aggregation, with D_H values comparable to those obtained for the freshwater algal medium (TG201). However, as suggested by the PDI and ζ_P values, together with D_H values obtained from intensity (Table S3†), AgNP3MPS suspension stability is partially affected by the increased complexity of LB and cDMEM, compared to TG201, which probably results in two size populations: fewer big aggregates

Table 1 Hydrodynamic diameter (D_H), polydispersity index (PDI), and ζ-potential (ζ_P) of AgNPcitLcys and AgNP3MPS resuspended at a concentration of 100 mg L^{-1} in different media: Milli-Q water, freshwater algal medium (TG201), bacterial medium (LB), cellular medium (cDMEM), and marine water algal medium (F/2). Hydrodynamic diameter values are reported as volume, as described in several studies on metal nanoparticles.[39–41] Tests were carried out at 25 °C. Data are shown as mean ± SD

	AgNPcitLcys					AgNP3MPS				
	Milli-Q	TG201	LB	cDMEM	F/2	Milli-Q	TG201	LB	cDMEM	F/2
D_H (nm) volume	12.5 ± 1	17 ± 14	671 ± 4	450 ± 20	862 ± 26	2 ± 1	5 ± 2	7 ± 9	7 ± 1	204 ± 2
PDI	0.3	0.3	0.1	0.3	0.3	0.4	0.6	0.4	0.5	0.6
ζ_P (mV)	−42 ± 2	−25 ± 0.3	−13 ± 0.3	−9.8 ± 0.5	−0.4 ± 2	−33 ± 2.8	−37 ± 3	−7.6 ± 0.5	−9.6 ± 1	−6 ± 3

(300–400 nm) and many small aggregates/single particles (20–30, 2–3 nm), as also suggested by DLS size distribution graphs (Fig. S1†).

As the TEM images show (Fig. 1), for both AgNPs, larger aggregates are formed in F/2 (40 ‰) (Fig. 1e and f), while TG201 caused a limited increase in D_H (Fig. 1c and d).

Dissolution also was affected by the suspension media, as previously observed for AgNPcitLcys.[42] In algal media only, a very low amount of Ag was released from both AgNPcitLcys and AgNP3MPS (<1% of nominal AgNP concentration) (Table 2), especially if compared to other AgNP batches.[43,44] Such a phenomenon can be ascribed to the specific coatings (citLcys or 3MPS) that might affect Ag dissolution rate. In agreement with the literature,[43] we found that the higher the salinity of water media, the greater the Ag release. Both AgNPs showed the maximum release in F/2, with 0.83% and 0.16% of nominal AgNP concentration for AgNPcitLcys and AgNP3MPS, respectively. Ag release increased with incubation time (from 1 to 72 h), except for AgNPcitLcys in the TG201 medium, where the dissolution rate was very low and showed a slight decrease between time points (1–72 h). This phenomenon might be attributed to a partial adhesion of Ag ions to the walls of the plastic tube in which the solutions were kept for 72 h under constant shaking, in agreement with Malysheva *et al.*,[13] or to an interaction of the (very few) released ions with the citLcys coating.

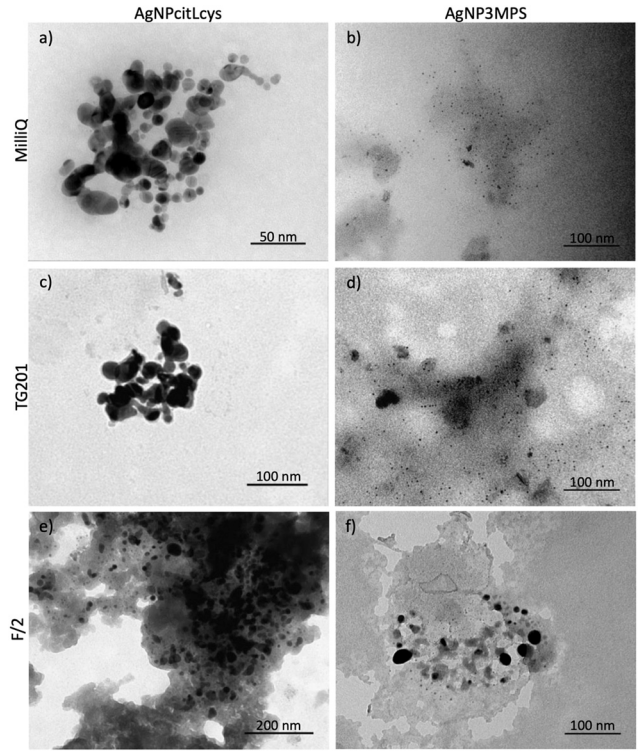

Fig. 1 TEM images of AgNPcitLcys and AgNP3MPS in Milli-Q water (a and b), TG201 (c and d) and F/2 (e and f).

A different scenario was found for protein-rich media. Because of the complexity of such media, some criticalities have arisen for the evaluation of Ag release using the selected separation protocol (3 kDa filtration). This was first noted for LB medium; therefore, the analysis was not performed in cDMEM.

In fact, after 1 h of incubation in LB medium only, a small yet detectable amount of Ag was measured for both AgNPs (0.027% and 0.0025% of nominal AgNP concentrations for, respectively, AgNPcitLcys and AgNP3MPS) (Table 2). However, after 24 h of incubation, the Ag concentration drastically decreased to values close to zero for both AgNPs.

Indeed, LB is a nutrient-rich microbial broth containing peptides, aminoacids, and carbohydrates (Table S1†), including tryptone (*i.e.*, a mix of peptides generated by the enzymatic digestion of casein) and yeast extract. The method used to separate AgNPs from the aqueous solution prior to Ag analysis requires a filtration step through a 3 kDa membrane filter. The adoption of this method was made necessary by the AgNPs' small size and was selected, as opposed to centrifugation, to ensure the total removal of AgNPs. Since metal analysis requires the addition of HNO_3 to the samples prior to measurement, even a small amount of AgNP left in solution after centrifugation would completely impair the purpose of the analysis. However, some components of LB medium might be able bind and seize metal ions[45] and, if retained by the filter, would reduce the amount of Ag in solution, as observed. The data of Ag recovery (Table S4†), obtained by adding $AgNO_3$ to LB medium in the absence of AgNPs, support such hypothesis showing a total removal of Ag upon filtration, as opposed to alga media. The fact that AgNP dissolution in LB medium appears to decrease with increasing incubation time might be ascribed to the kinetic of dissolution/bonding with biomolecules, which might take more than 1 h to reach equilibrium.

Table 2 Total Ag (μg L^{-1}) measured after incubation (1 and 72 h for microalgae and 1 and 24 h for bacteria) and filtration of 60 mg L^{-1} of AgNPcitLcys or AgNP3MPS in TG201 and F/2 and of 256 mg L^{-1} of AgNPcitLcys or AgNP3MPS in the LB medium

	Medium	1 h	24/72 h
AgNPcitLcys	TG201 (60 mg L^{-1})	2.08 ± 0.06 (0.0034%)	1.33 ± 0.1 (0.0022%)
	LB (256 mg L^{-1})	70.59 ± 1.57 (0.027%)	1.64 ± 0.05 (0.00064%)
	F/2 (60 mg L^{-1})	239.01 ± 1.83 (0.4%)	500.75 ± 14.5 (0.83%)
AgNP3MPS	TG201 (60 mg L^{-1})	11.01 ± 0.12 (0.018%)	18.42 ± 0.62 (0.03%)
	LB (256 mg L^{-1})	6.49 ± 0.14 (0.0025%)	0.61 ± 0.07 (0.00024%)
	F/2 (60 mg L^{-1})	59.15 ± 0.98 (0.1%)	95.16 ± 2.87 (0.16%)

Two options, which might also simultaneously occur, were selected to describe such findings: (i) dissolved Ag ions are bonded by free peptides and carbohydrates of LB medium, which are retained during filtration, and/or (ii) free peptides and carbohydrates of LB medium directly bind to AgNPs, forming the so-called protein corona and reducing (or preventing) AgNP dissolution. NP interaction with biomolecules, resulting in the formation of a protein-corona, is well documented in the literature, also for other type of NPs.[46–49] The adsorption of proteins on the surface of AgNPs can modify their surface properties and, therefore, their biological identity can be substantially altered after suspension in protein-rich media.[46–50] According to this, one-dimensional polyacrylamide gel electrophoresis (1D-PAGE) was performed after AgNPs incubation in protein-rich growth media, LB and cDMEM. The selected procedure allows for the detection of the "hard corona", the layer of biomolecules that are tightly bound to NP surface, while the "soft corona", more loosely bound, was presumably washed away.[47]

Interestingly, 1D-PAGE revealed the formation of a hard corona around AgNPcitLcys after incubation in both protein-rich media, while no biomolecules formed a stable bond with AgNP3MPS (Fig. 3). This was confirmed by TEM (Fig. 2a and b), showing AgNPcitLcys being embedded into a polymeric matrix, as opposed to AgNP3MPS (Fig. 2c and d), which appeared to be free from the bonded biomolecules/matrix.

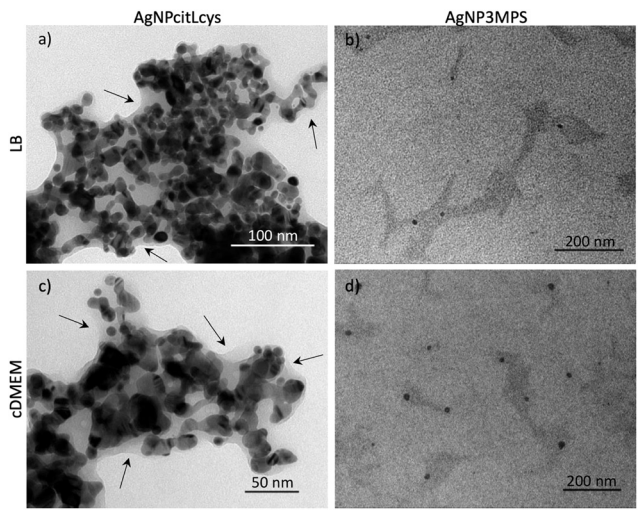

Fig. 2 TEM images of AgNPcitLcys (a and c) and AgNP3MPS (b and d) after incubation in the LB medium (a and b) and cDMEM (c and d) for 2 h, centrifugation, and washing 3 times in PBS. Arrows indicate the protein corona formed onto AgNPcitLcys upon incubation in protein-rich media.

Corona formation after AgNP suspension in protein-rich media is widely reported in the literature,[51–55] but fewer data are available about the lack of a stable interaction with medium elements, leading to the absence of a protein corona. Protein–NP interaction is driven by intermolecular forces occurring at the bio–nano interface and is virtually influenced by an enormous number of variables, such as NP surface curvature and the relative amount of β-sheets and α-helices in encountered proteins.[54–56] The abundance of citrate molecules as AgNP coating, for instance, was shown to promote protein adsorption, while their replacement with alkanethiol molecules ((11-mercaptoundecyl)hexa(ethylene glycol)) substantially increased the resistance to protein adsorption.[57]

Overall, our observations disclose how the surface capping drives the AgNPs' aggregation behaviour in water media, the release of Ag ions and the potential of AgNPs to interact with biomolecules, potentially affecting their biological effect.

3.2. AgNPs (eco)toxicity towards microorganisms and mammalian cells

The (eco)toxicity of AgNPcitLcys and AgNP3MPS was evaluated against unicellular microorganisms, such as Gram-negative bacteria (*E. coli*), freshwater (*R. subcapitata*) and marine (*P. tricornutum*) microalgae, and against mammalian cells of human (HeLa) and murine (L929) origin.

As depicted in Fig. 4, AgNPs functionalized with citLcys possess good antibacterial activity against Gram-negative *E. coli* (≈50% bacterial growth inhibition) only at concentrations ≥256 mg L^{-1}. Conversely, AgNP3MPS did not affect bacterial growth at any concentration tested (up to 256 mg L^{-1}). As expected, $AgNO_3$ showed total inhibition of growth already at 8 mg L^{-1} (Fig. S3†) and an EC_{50} ≈ 4.43 mg L^{-1} (Table 3).

Both AgNPs showed a lower toxicity to *E. coli* compared to that reported in the literature.[20,58] In particular, the small size as that of AgNP3MPS (<3 nm) is known to represent a key element for antibacterial potential as it allows a greater interaction with cells, which is a trigger to the onset of toxicity.[59] In fact, the usually high antimicrobial potential of

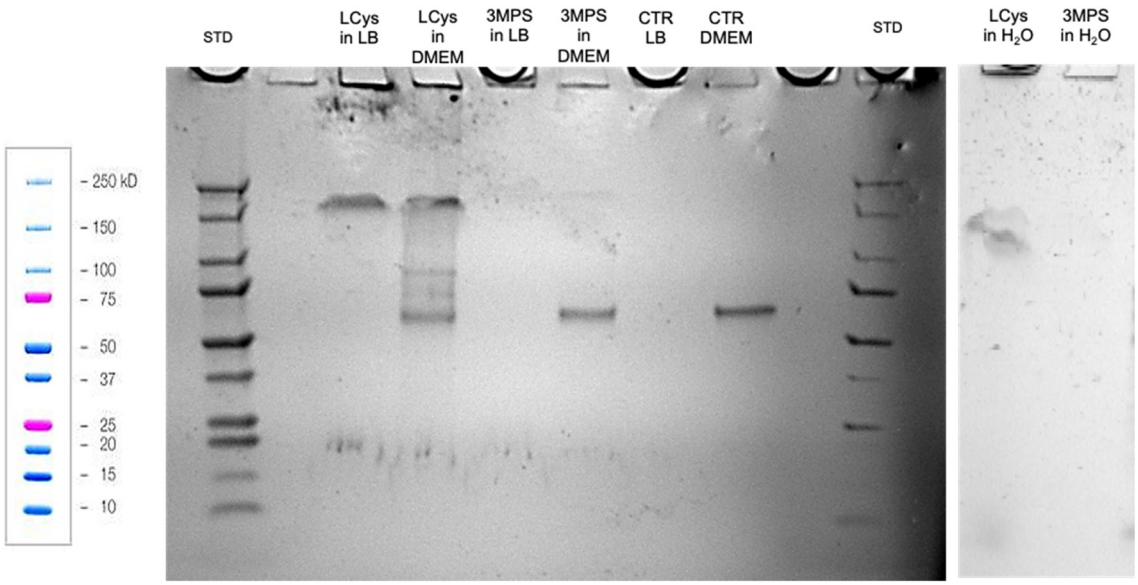

Fig. 3 1D-PAGE of the protein fraction of the protein corona recovered from AgNPs exposed to different media.

AgNPs towards *E. coli* stands in their direct interaction with the bacterial wall, causing disturbances in charge distribution and a loss of membrane integrity.[18] This results in the formation of holes in the bacterial outer membrane, causing the entrance of AgNPs with consequent oxidation and dissolution inside the cytoplasm.[18,20] Therefore, based on our findings on the low *E. coli* toxicity, we can speculate that a reduced (or absent) interaction between both AgNP3MPS and AgNPcitLcys and bacteria occurred.

The formation of a protein corona around the AgNPcitLcys might have reduced the direct interaction with bacterial cells, allowing the onset of toxicity only at very high concentrations (256 mg L^{-1}). Conversely, the coating of AgNP3MPS could be responsible for the absence of *E. coli* toxicity by determining a reduced/absent interaction with bacterial cells. Medium components might as well be playing a role by bonding released Ag ions, reducing their bioavailability and toxicity. Hence, both citLcys and 3MPS coatings, probably as a result of different mechanisms, determined a low antibacterial activity of the AgNPs.

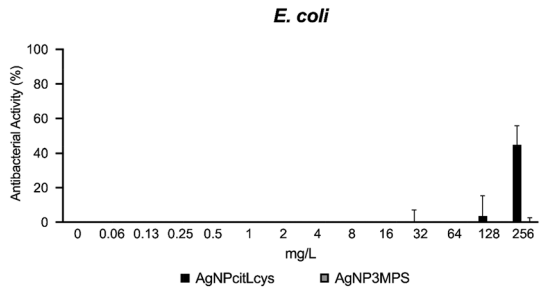

Fig. 4 Comparative antibacterial activity (%) of AgNPcitLcys (black bars) and AgNP3MPS (grey bars) against *E. coli*. Data are expressed as mean ± SD ($n \geq 3$).

A different trend was observed for microalgae, even between freshwater and marine species (Fig. 5). Indeed, the freshwater *R. subcapitata* showed higher sensitivity to both AgNPs compared to the marine *P. tricornutum*, already at lower exposure concentrations (1–5 mg L^{-1}). It is worth noting that these concentration are still quite high if compared to predicted environmental concentrations (PECs) for AgNP in surface waters (1–100 μg L^{-1}).[10,11] AgNP3MPS resulted to be the most toxic for *R. subcapitata*, with a linear increase in growth inhibition up to more than 80% (60 mg L^{-1}), while AgNPcitLcys were less toxic, reaching a maximum inhibition of 38.6% (60 mg L^{-1}) compared to the control. Conversely, *P. tricornutum* did not show toxic effects up to 60 mg L^{-1} of both AgNPs. Similarly, $AgNO_3$ showed higher toxicity to *R. subcapitata* (EC_{50} = 6.74 μg Ag L^{-1}) compared to *P. tricornutum* (EC_{50} > 1 mg Ag L^{-1}) (Fig. S3†).

Besides a higher sensitivity of *R. subcapitata* to Ag exposure, the chemistry of exposure media probably also played a role in the observed difference in ecotoxicity, by influencing Ag speciation. In fact, the high salinity of F/2 (*P. tricornutum* growth medium) and the presence of natural organic matter (NOM) likely caused the reduction of bioavailable Ag by (i) formation of Cl–Ag complexes and (ii) bonding of Ag ions to NOM macromolecules, rich in SH–groups.[43,60] On the other hand, TG201 (*R. subcapitata* growth medium), having very few dissolved salts and no NOM, offered no mitigation against Ag ion toxicity. In both cases, the observed toxicity for AgNPcitLcys and AgNP3MPS towards microalgae is low if compared to literature data,[12,61–64] as already shown for only AgNPcitLcys.[24,42,65]

However, dissolved Ag might not be the only factor involved in the effects of AgNP towards microalgae. In fact, if we consider algal growth inhibition percentages together with AgNP dissolution data, we can see that the effects of AgNP3MPS can be predicted based on dissolved Ag levels:

Table 3 EC_{50} values calculated for *R. subcapitata*, *P. tricornutum*, and *E. coli* exposed to AgNPcitLcys, AgNP3MPS and $AgNO_3$

EC_{50}	*R. subcapitata*	*P. tricornutum*	*E. coli*	HeLa	*L929*
AgNPcitLcys	>60 mg L^{-1}	>60 mg L^{-1}	>256 mg L^{-1}	>256 mg L^{-1}	>256 mg L^{-1}
AgNP3MPS	7.57 mg L^{-1} (CI 95% 6.5–8.61)	>60 mg L^{-1}	>256 mg L^{-1}	>256 mg L^{-1}	>256 mg L^{-1}
$AgNO_3$	6.74 μg L^{-1} (CI 95% 6.18–7.36)	>1 mg L^{-1}	4.43 mg L^{-1}	3.79 mg mL^{-1}	7.45 mg mL^{-1}

18.42 μg Ag L^{-1} caused an 80% inhibition of growth in *R. subcapitata* while no effect is observed in *P. tricornutum* for a 95.16 μg L^{-1} of dissolved Ag, as expected based on $AgNO_3$ exposure (Fig. S3†). Instead, the inhibition of growth caused by AgNPcitLcys does not seem to follow a rationale based on dissolution percentage: a 38.6% inhibition of growth of *R. subcapitata* was observed at a dissolved Ag value of 1.33 μg L^{-1}, too low to explain such toxicity. On the other hand, no effect is observed for *P. tricornutum* at a dissolved Ag value of 500 μg L^{-1}, which would be enough to cause an inhibition based on $AgNO_3$ ecotoxicity data.

Such discrepancies suggest that AgNPcitLcys and AgNP3MPS act differently towards algal cells, with AgNP3MPS toxicity being more closely related to dissolution compared to AgNPcitLcys, whose effects seem to be influenced by other factors. Since the citLcys coating can drive the interaction with biomolecules, it also might enhance the interaction with algal cells, possibly leading to AgNP internalization. Hence, AgNP toxicity towards microalgae is not solely caused by ion release but can also be directly influenced by the coating type.

To further investigate AgNP effect on different cell types and exposure media, we tested two different mammalian cell lines, namely, HeLa and L929 cells, from human and murine origin. Interestingly, the cytotoxic effects of AgNPcitLcys and AgNP3MPS on HeLa and L929 cells were low-to-negligible as lower than 30% at all tested concentrations (Fig. 6). According to the ISO 10993-5 (ref. 37) standard norm, both AgNPcitLcys and AgNP3MPS were far from being toxic on mammalian cells. Conversely, as expected, $AgNO_3$ displayed a concentration-dependent cytotoxicity, resulting in effective concentrations of 4 mg L^{-1} and 8 mg L^{-1} for L929 and HeLa cells, respectively. Again, our findings show a lower toxicity of AgNPcitLcys and AgNP3MPS compared to the literature,[66–69] suggesting a protective role of both capping types also for mammalian cells. For instance, in the study by Pem *et al.*,[69] AgNPs with a cysteine coating (Cys-AgNPs) significantly reduced L929 cell viability starting from 10 mg L^{-1}, while no toxicity was observed in this study up to 256 mg L^{-1} for AgNPcitLcys. The formation of the protein corona around AgNPcitLcys probably contributes to the lower toxicity observed as it could be reducing (or impede) cellular uptake, different from what observed by Pem *et al.*[69] for Cys-AgNPs.

3.3. The role of the coating

Surface functionalization plays a key role for AgNP applications, especially those involving environmental protection. Often, multiple functionalizing molecules are introduced onto the surface of the nanosilver to induce different capacities, such as hydrophilicity and, at the same time, high selectivity or antibacterial activity. In this case, AgNPcitLcys and AgNP3MPS present, respectively, a double

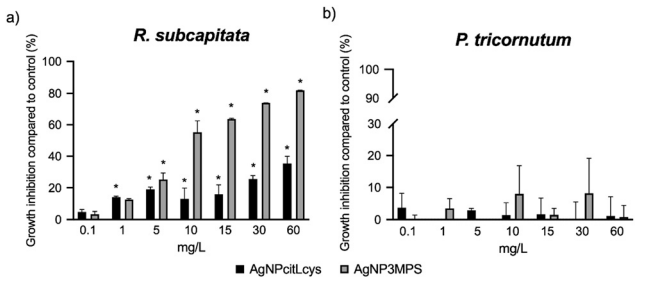

Fig. 5 Comparative growth inhibition rate evaluated on a) *R. subcapitata* and b) *P. tricornutum* upon exposure to AgNPcitLcys (black bars) and AgNP3MPS (grey bars) for 72 h. Data are expressed as mean ± SD ($n \geq 3$). Columns marked with * are statistically different from the control ($p < 0.05$).

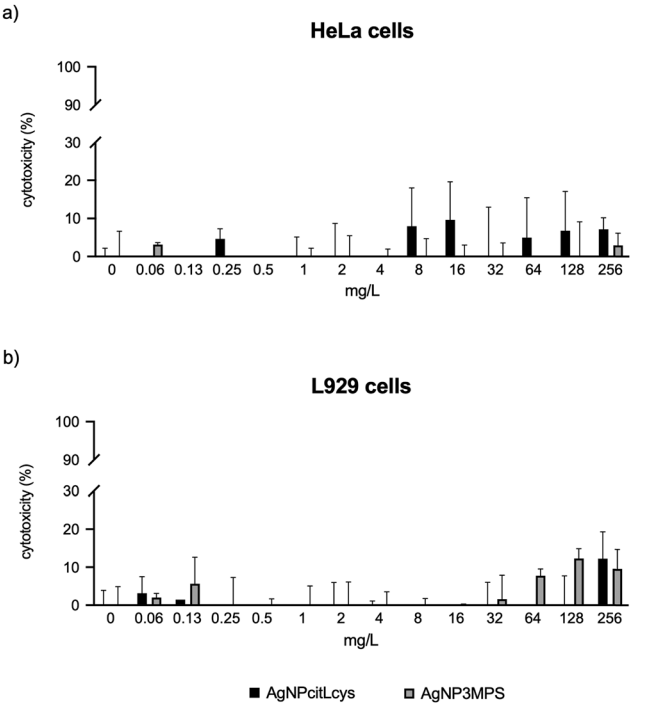

Fig. 6 Comparative cytotoxicity of AgNPcitLcys (black bars) and AgNP3MPS (grey bars) evaluated on a) HeLa and b) L929 cell lines. AgNPcitLcys and AgNP3MPS were incubated with cells for 24 h. Data are expressed as mean ± SD. Statistical analysis showed no significant differences between treatments and controls ($p > 0.05$).

functionalization with a hydrophilic agent (cit) and a molecule that induces selectivity for Hg(II) (Lcys), and a capping agent that guarantees both hydrophilicity and selectivity for Ni(II) (3MPS). This translates not only into different chemical–physical properties, as seen in the previous paragraphs, but also into different biological effects.

In summary, only *R. subcapitata* suffered the exposure to both AgNPs, AgNP3MPS more than AgNPcitLcys, while *E. coli* experienced a low toxicity and only upon exposure to high AgNPcitLcys concentrations (256 mg L^{-1}). The results obtained for *E. coli* were unexpected since the smaller size and the absence of a protein corona made AgNP3MPS the best candidate for a higher antimicrobial activity.[18,59] However, if the 3MPS coating would not encourage the interaction with cells, the only antimicrobial mechanism left for AgNP3MPs would be the release of Ag ions. In this scenario, the absence of toxicity of AgNP3MPS towards both *E. coli* and mammalian cells could be explained with Ag ion bonding by proteins and polysaccharides of the growth media. At the same time, this is confirmed by what is seen for *R. subcapitata* where, in the absence of macromolecules able to seize Ag ions, AgNP3MPS result in toxicity. Conversely, since AgNPcitLcys reduce *R. subcapitata* growth even with a dissolution close to zero, we can hypothesize that the citLcys coating encourages the interaction with cells, leading to the onset of a nano-size related toxicity. Where the nano-size is lost due to aggregation, as in F/2 medium, or AgNPcitLcys surface is altered by corona formation, as in LB and cDMEM media, the exposure outcome is different: no effect is seen for *P. tricornutum*, also thanks to its siliceous cell wall, and a low-to-no toxicity is observed for *E. coli* and mammalian cells, whose direct interaction with AgNPcitLcys is hindered (or lowered) by the protein corona.

4. Conclusions

Our study aimed at comparing the (eco)toxicity of differently coated AgNPs towards unicellular organisms, such as bacteria, freshwater and marine microalgae, and mammalian cell-lines, of human and murine origin. The citLcys coating reduced AgNP dissolution, promoted the interaction with macromolecules and much likely drove AgNP affinity for algal surface, suggesting the occurrence of a nano-size-related ecotoxicity. On the other hand, 3MPS coating allowed a higher degree of AgNP dissolution and caused no interaction with macromolecules, resulting in a higher ecotoxicity when mitigating factors for Ag bioavailability (*e.g.*, Cl ions or macromolecules) were absent. Our findings show how surface capping rules AgNP interaction with biomolecules, driving the AgNP ability to establish an interaction with cells, influencing the exposure outcome.

Author contributions

Conceptualization: A. B., I. C., N. B., G. C., I. V.; methodology: A. B., N. B., F. B., L. B.; investigation: A. B., N. B., C. F., G. P., E. P.; formal analysis: A. B., N. B.; data curation: A. B., N. B., I. C., G. C.; project administration: I. C., G. C.; funding acquisition: I. C., I. V., G. C., P. L.; writing – original draft: A. B., I. C., N. B., G. C., I. V.; writing – revision: A. B., I. C., N. B., G. C., I. V. All authors have read and agreed to the published version of the manuscript.

Conflicts of interest

There are no conflicts of interest to declare.

Acknowledgements

Project funded under the National Recovery and Resilience Plan (NRRP), Mission 4 Component 2 Investment 1.4 – Call for tender No. 3138 of 16 December 2021, rectified by Decree n.3175 of 18 December 2021 of Italian Ministry of University and Research funded by the European Union – NextGenerationEU; Award Number: Project code CN_00000033, Concession Decree No. 1034 of 17 June 2022 adopted by the Italian Ministry of University and Research, CUP B63C22000650007, Project Title "National Biodiversity Future Center – NBFC". The authors of the Sciences Department of Roma Tre University thank the MUR (MIUR-Italy Departments of Excellence 2023, Article 1, Comma 314–337, Low 232/2016) and Rome Technopole Project CUP: F83B22000040006. This research was inspired by Regione Lazio, through "Gruppi di ricerca 2020"-POR FESR Lazio 2014-2020 (prot. GeCoWEB n. A0375-2020-36521, CUP E85F21002440002).

References

1 S. S. Salem, E. N. Hammad, A. A. Mohamed and W. El-Dougdoug, A comprehensive review of nanomaterials: types, synthesis, characterization, and applications, *Biointerface Res. Appl. Chem.*, 2022, **13**, 2023.
2 A. Fiorati, A. Bellingeri, C. Punta, I. Corsi and I. Venditti, Silver Nanoparticles for Water Pollution Monitoring and Treatments: Ecosafety Challenge and Cellulose-Based Hybrids Solution, *Polymers*, 2020, **12**, 1635.
3 I. Corsi, I. Venditti, F. Trotta and C. Punta, Environmental safety of nanotechnologies: The eco-design of manufactured nanomaterials for environmental remediation, *Sci. Total Environ.*, 2023, **864**, 161181.
4 L. Rizzello and P. P. Pompa, Nanosilver-based antibacterial drugs and devices: mechanisms, methodological drawbacks, and guidelines, *Chem. Soc. Rev.*, 2014, **43**, 1501–1518.
5 A. Ravindran, P. Chandran and S. S. Khan, Biofunctionalized silver nanoparticles: advances and prospects, *Colloids Surf., B*, 2013, **105**, 342–352.
6 A. Bellingeri, F. Bertelà, L. Burratti, A. Calantropio, C. Battocchio, P. Lupetti, E. Paccagnini, G. Iucci, M. Marsotto and P. Prosposito, Detection of Fe (III) ion based on bifunctionalized silver nanoparticles: Sensitivity, selectivity and environmental safety, *Mater. Chem. Phys.*, 2024, **313**, 128671.
7 A. Rossi, M. Cuccioloni, L. R. Magnaghi, R. Biesuz, M. Zannotti, L. Petetta, M. Angeletti and R. Giovannetti,

Optimizing the Heavy Metal Ion Sensing Properties of Functionalized Silver Nanoparticles: The Role of Surface Coating Density, *Chemosensors*, 2022, **10**, 483.

8 G. Shumi, T. B. Demissie, R. Eswaramoorthy, R. F. Bogale, G. Kenasa and T. Desalegn, Biosynthesis of Silver Nanoparticles Functionalized with Histidine and Phenylalanine Amino Acids for Potential Antioxidant and Antibacterial Activities, *ACS Omega*, 2023, **8**, 24371–24386.

9 L. Li, M. Stoiber, A. Wimmer, Z. Xu, C. Lindenblatt, B. Helmreich and M. Schuster, To what extent can full-scale wastewater treatment plant effluent influence the occurrence of silver-based nanoparticles in surface waters?, *Environ. Sci. Technol.*, 2016, **50**, 6327–6333.

10 P. Cervantes-Avilés, Y. Huang and A. A. Keller, Multi-technique approach to study the stability of silver nanoparticles at predicted environmental concentrations in wastewater, *Water Res.*, 2019, **166**, 115072.

11 A. Lazareva and A. A. Keller, Estimating potential life cycle releases of engineered nanomaterials from wastewater treatment plants, *ACS Sustainable Chem. Eng.*, 2014, **2**, 1656–1665.

12 M. Kleiven, A. Macken and D. H. Oughton, Growth inhibition in Raphidocelis subcapita–Evidence of nanospecific toxicity of silver nanoparticles, *Chemosphere*, 2019, **221**, 785–792.

13 A. Malysheva, N. Voelcker, P. E. Holm and E. Lombi, Unraveling the complex behavior of AgNPs driving NP-cell interactions and toxicity to algal cells, *Environ. Sci. Technol.*, 2016, **50**, 12455–12463.

14 J. Zhang, L. Shen, Q. Xiang, J. Ling, C. Zhou, J. Hu and L. Chen, Proteomics reveals surface electrical property-dependent toxic mechanisms of silver nanoparticles in Chlorella vulgaris, *Environ. Pollut.*, 2020, 114743.

15 S. Schiavo, N. Duroudier, E. Bilbao, M. Mikolaczyk, J. Schäfer, M. Cajaraville and S. Manzo, Effects of PVP/PEI coated and uncoated silver NPs and PVP/PEI coating agent on three species of marine microalgae, *Sci. Total Environ.*, 2017, **577**, 45–53.

16 I. Kalantzi, K. Mylona, C. Toncelli, T. D. Bucheli, K. Knauer, S. A. Pergantis, P. Pitta, A. Tsiola and M. Tsapakis, Ecotoxicity of silver nanoparticles on plankton organisms: a review, *J. Nanopart. Res.*, 2019, **21**, 65.

17 J. Beddow, B. Stolpe, P. A. Cole, J. R. Lead, M. Sapp, B. P. Lyons, I. Colbeck and C. Whitby, Nanosilver inhibits nitrification and reduces ammonia-oxidising bacterial but not archaeal amoA gene abundance in estuarine sediments, *Environ. Microbiol.*, 2017, **19**, 500–510.

18 S. P. Theofilou, C. Antoniou, L. Potamiti, A. Hadjisavvas, M. Panayiotidis, P. G. Savva, C. Costa and V. Fotopoulos, Immobilized Ag-nanoparticles (iNPs) for environmental applications: Elucidation of immobilized silver-induced inhibition mechanism of Escherichia coli, *J. Environ. Chem. Eng.*, 2021, **9**, 106001.

19 M. B. Faiz, R. Amal, C. P. Marquis, E. J. Harry, G. A. Sotiriou, S. A. Rice and C. Gunawan, Nanosilver and the microbiological activity of the particulate solids versus the leached soluble silver, *Nanotoxicology*, 2018, **12**, 263–273.

20 I. Sondi and B. Salopek-Sondi, Silver nanoparticles as antimicrobial agent: a case study on E. coli as a model for Gram-negative bacteria, *J. Colloid Interface Sci.*, 2004, **275**, 177–182.

21 A. Kędziora, M. Speruda, E. Krzyżewska, J. Rybka, A. Łukowiak and G. Bugla-Płoskońska, Similarities and differences between silver ions and silver in nanoforms as antibacterial agents, *Int. J. Mol. Sci.*, 2018, **19**, 444.

22 A. Sukhanova, S. Bozrova, P. Sokolov, M. Berestovoy, A. Karaulov and I. Nabiev, Dependence of nanoparticle toxicity on their physical and chemical properties, *Nanoscale Res. Lett.*, 2018, **13**, 1–21.

23 I. Venditti, G. Testa, F. Sciubba, L. Carlini, F. Porcaro, C. Meneghini, S. Mobilio, C. Battocchio and I. Fratoddi, Hydrophilic metal nanoparticles functionalized by 2-Diethylaminoethanethiol: a close look at the metal–ligand interaction and interface chemical structure, *J. Phys. Chem. C*, 2017, **121**, 8002–8013.

24 P. Prosposito, L. Burratti, A. Bellingeri, G. Protano, C. Faleri, I. Corsi, C. Battocchio, G. Iucci, L. Tortora and V. Secchi, Bifunctionalized Silver Nanoparticles as Hg2+ Plasmonic Sensor in Water: Synthesis, Characterizations, and Ecosafety, *Nanomaterials*, 2019, **9**, 1353.

25 I. Schiesaro, L. Burratti, C. Meneghini, I. Fratoddi, P. Prosposito, J. Lim, C. Scheu, I. Venditti, G. Iucci and C. Battocchio, Hydrophilic silver nanoparticles for Hg (II) detection in water: Direct evidence for mercury–silver interaction, *J. Phys. Chem. C*, 2020, **124**, 25975–25983.

26 F. Bertelà, M. Marsotto, C. Meneghini, L. Burratti, V.-A. Maraloiu, G. Iucci, I. Venditti, P. Prosposito, V. D'Ezio and T. Persichini, Biocompatible Silver Nanoparticles: Study of the Chemical and Molecular Structure, and the Ability to Interact with Cadmium and Arsenic in Water and Biological Properties, *Nanomaterials*, 2021, **11**, 2540.

27 F. Mochi, L. Burratti, I. Fratoddi, I. Venditti, C. Battocchio, L. Carlini, G. Iucci, M. Casalboni, F. De Matteis and S. Casciardi, Plasmonic sensor based on interaction between silver nanoparticles and Ni2+ or Co2+ in water, *Nanomaterials*, 2018, **8**, 488.

28 I. Schiesaro, C. Battocchio, I. Venditti, P. Prosposito, L. Burratti, P. Centomo and C. Meneghini, Structural characterization of 3d metal adsorbed AgNPs, *Phys. E*, 2020, **123**, 114162.

29 D. Maiolo, J. Colombo, J. Beretta, C. Malloggi, G. Candiani and F. B. Bombelli, The polyplex, protein corona, cell interplay: Tips and drawbacks, *Colloids Surf., B*, 2018, **168**, 60–67.

30 ISO/20776-1, Susceptibility testing of infectious agents and evaluation of performance of antimicrobial susceptibility test devices - Part 1: Broth micro-dilution reference method for testing the in vitro activity of antimicrobial agents against rapidly growing aerobic bacteria involved in infectious diseases (ISO 20776-1:2019, including Corrected version 2019-12)).

31 A. Rossetti, N. Bono, G. Candiani, F. Meneghetti, G. Roda and A. Sacchetti, Synthesis and Antimicrobial Evaluation of

Novel Chiral 2-Amino-4, 5, 6, 7-tetrahydrothieno [2, 3-c] pyridine Derivatives, *Chem. Biodiversity*, 2019, **16**, e1900097.
32 J. Campbell, High-throughput assessment of bacterial growth inhibition by optical density measurements, *Curr. Protoc. Chem. Biol.*, 2010, **2**, 195–208.
33 OECD and 201, (2011) Test No. 201: Freshwater Alga and Cyanobacteria, Growth Inhibition Test, OECD Guidelines for the Testing of Chemicals, Section 2, OECD Publishing, Paris, DOI: **10.1787/9789264069923-en**.
34 ISO/10253, Water quality — Marine algal growth inhibition test with *Skeletonema costatum* and *Phaeodactylum tricornutum*).
35 C. Resgalla Jr, F. Poleza, R. Souza, M. Máximo and C. Radetski, Evaluation of effectiveness of EDTA and sodium thiosulfate in removing metal toxicity towards sea urchin embryo-larval applying the TIE, *Chemosphere*, 2012, **89**, 102–107.
36 P. P. Leal, C. L. Hurd, S. G. Sander, E. Armstrong and M. Y. Roleda, Copper ecotoxicology of marine algae: a methodological appraisal, *Chem. Ecol.*, 2016, **32**, 786–800.
37 ISO/10993-5, Biological evaluation of medical devices — Part 5: Tests for in vitro cytotoxicity).
38 P. Prosposito, F. Mochi, E. Ciotta, M. Casalboni, F. De Matteis, I. Venditti, L. Fontana, G. Testa and I. Fratoddi, Hydrophilic silver nanoparticles with tunable optical properties: Application for the detection of heavy metals in water, *Beilstein J. Nanotechnol.*, 2016, **7**, 1654–1661.
39 J. Lim, S. P. Yeap, H. X. Che and S. C. Low, Characterization of magnetic nanoparticle by dynamic light scattering, *Nanoscale Res. Lett.*, 2013, **8**, 1–14.
40 R. De Angelis, I. Venditti, I. Fratoddi, F. De Matteis, P. Prosposito, I. Cacciotti, L. D'Amico, F. Nanni, A. Yadav and M. Casalboni, From nanospheres to microribbons: Self-assembled Eosin Y doped PMMA nanoparticles as photonic crystals, *J. Colloid Interface Sci.*, 2014, **414**, 24–32.
41 C. Cametti, I. Fratoddi, I. Venditti and M. Russo, Dielectric relaxations of ionic thiol-coated noble metal nanoparticles in aqueous solutions: electrical characterization of the interface, *Langmuir*, 2011, **27**, 7084–7090.
42 A. Bellingeri, M. Scattoni, I. Venditti, C. Battocchio, G. Protano and I. Corsi, Ecologically based methods for promoting safer nanosilver for environmental applications, *J. Hazard. Mater.*, 2022, 129523.
43 R. A. D. Lish, S. A. Johari, M. Sarkheil and I. J. Yu, On how environmental and experimental conditions affect the results of aquatic nanotoxicology on brine shrimp (Artemia salina): A case of silver nanoparticles toxicity, *Environ. Pollut.*, 2019, **255**, 113358.
44 F. Wu, B. J. Harper and S. L. Harper, Differential dissolution and toxicity of surface functionalized silver nanoparticles in small-scale microcosms: impacts of community complexity, *Environ. Sci.: Nano*, 2017, **4**, 359–372.
45 S. Ramamoorthy and D. Kushner, Binding of mercuric and other heavy metal ions by microbial growth media, *Microb. Ecol.*, 1975, **2**, 162–176.
46 A. Lesniak, F. Fenaroli, M. P. Monopoli, C. Åberg, K. A. Dawson and A. Salvati, Effects of the presence or absence of a protein corona on silica nanoparticle uptake and impact on cells, *ACS Nano*, 2012, **6**, 5845–5857.
47 M. P. Monopoli, A. S. Pitek, I. Lynch and K. A. Dawson, in *Nanomaterial interfaces in biology*, Springer, 2013, pp. 137–155.
48 Y. Hayashi, T. Miclaus, C. Scavenius, K. Kwiatkowska, A. Sobota, P. Engelmann, J. J. Scott-Fordsmand, J. J. Enghild and D. S. Sutherland, Species differences take shape at nanoparticles: protein corona made of the native repertoire assists cellular interaction, *Environ. Sci. Technol.*, 2013, **47**, 14367–14375.
49 G. Grassi, E. Gabellieri, P. Cioni, E. Paccagnini, C. Faleri, P. Lupetti, I. Corsi and E. Morelli, Interplay between extracellular polymeric substances (EPS) from a marine diatom and model nanoplastic through eco-corona formation, *Sci. Total Environ.*, 2020, **725**, 138457.
50 M. Barbalinardo, F. Caicci, M. Cavallini and D. Gentili, Protein corona mediated uptake and cytotoxicity of silver nanoparticles in mouse embryonic fibroblast, *Small*, 2018, **14**, 1801219.
51 A. P. Ault, D. I. Stark, J. L. Axson, J. N. Keeney, A. D. Maynard, I. L. Bergin and M. A. Philbert, Protein corona-induced modification of silver nanoparticle aggregation in simulated gastric fluid, *Environ. Sci.: Nano*, 2016, **3**, 1510–1520.
52 A. Tomak, B. Yilancioglu, D. Winkler and C. O. Karakus, Protein corona formation on silver nanoparticles under different conditions, *Colloids Surf., A*, 2022, **651**, 129666.
53 S. Argentiere, C. Cella, M. Cesaria, P. Milani and C. Lenardi, Silver nanoparticles in complex biological media: assessment of colloidal stability and protein corona formation, *J. Nanopart. Res.*, 2016, **18**, 1–13.
54 J. H. Shannahan, X. Lai, P. C. Ke, R. Podila, J. M. Brown and F. A. Witzmann, Silver nanoparticle protein corona composition in cell culture media, *PLoS One*, 2013, **8**, e74001.
55 V. Gorshkov, J. A. Bubis, E. M. Solovyeva, M. V. Gorshkov and F. Kjeldsen, Protein corona formed on silver nanoparticles in blood plasma is highly selective and resistant to physicochemical changes of the solution, *Environ. Sci.: Nano*, 2019, **6**, 1089–1098.
56 A. E. Nel, L. Mädler, D. Velegol, T. Xia, E. M. Hoek, P. Somasundaran, F. Klaessig, V. Castranova and M. Thompson, Understanding biophysicochemical interactions at the nano-bio interface, *Nat. Mater.*, 2009, **8**, 543.
57 M. Barbalinardo, J. Bertacchini, L. Bergamini, M. S. Magarò, L. Ortolani, A. Sanson, C. Palumbo, M. Cavallini and D. Gentili, Surface properties modulate protein corona formation and determine cellular uptake and cytotoxicity of silver nanoparticles, *Nanoscale*, 2021, **13**, 14119–14129.
58 C. Baker, A. Pradhan, L. Pakstis, D. J. Pochan and S. I. Shah, Synthesis and antibacterial properties of silver nanoparticles, *J. Nanosci. Nanotechnol.*, 2005, **5**, 244–249.
59 J. R. Morones, J. L. Elechiguerra, A. Camacho, K. Holt, J. B. Kouri, J. T. Ramírez and M. J. Yacaman, The bactericidal effect of silver nanoparticles, *Nanotechnology*, 2005, **16**, 2346.

60 P. Li, M. Su, X. Wang, X. Zou, X. Sun, J. Shi and H. Zhang, Environmental fate and behavior of silver nanoparticles in natural estuarine systems, *J. Environ. Sci.*, 2020, **88**, 248–259.
61 M. Sendra, M. Yeste, J. Gatica, I. Moreno-Garrido and J. Blasco, Direct and indirect effects of silver nanoparticles on freshwater and marine microalgae (Chlamydomonas reinhardtii and Phaeodactylum tricornutum), *Chemosphere*, 2017, **179**, 279–289.
62 S. Lekamge, A. F. Miranda, C. Trestrail, B. Pham, A. S. Ball, R. Shukla and D. Nugegoda, The Toxicity of Nonaged and Aged Coated Silver Nanoparticles to Freshwater Alga Raphidocelis subcapitata, *Environ. Toxicol. Chem.*, 2019, **38**, 2371–2382.
63 S. Lekamge, A. F. Miranda, A. Abraham, A. S. Ball, R. Shukla and D. Nugegoda, The toxicity of coated silver nanoparticles to the alga Raphidocelis subcapitata, *SN Appl. Sci.*, 2020, **2**, 1–14.
64 R. Biba, K. Košpić, B. Komazec, D. Markulin, P. Cvjetko, D. Pavoković, P. Peharec Štefanić, M. Tkalec and B. Balen, Surface coating-modulated phytotoxic responses of silver nanoparticles in plants and freshwater green algae, *Nanomaterials*, 2022, **12**, 24.
65 A. Bellingeri, C. Battocchio, C. Faleri, G. Protano, I. Venditti and I. Corsi, Sensitivity of Hydra vulgaris to Nanosilver for Environmental Applications, *Toxics*, 2022, **10**, 695.
66 A. R. Gliga, S. Skoglund, I. O. Wallinder, B. Fadeel and H. L. Karlsson, Size-dependent cytotoxicity of silver nanoparticles in human lung cells: the role of cellular uptake, agglomeration and Ag release, *Part. Fibre Toxicol.*, 2014, **11**, 11.
67 X. Liu, K. Shan, X. Shao, X. Shi, Y. He, Z. Liu, J. A. Jacob and L. Deng, Nanotoxic effects of silver nanoparticles on normal HEK-293 cells in comparison to cancerous HeLa cell line, *Int. J. Nanomed.*, 2021, **16**, 753.
68 S. B. Nadhe, M. S. Tawre, S. Agrawal, B. A. Chopade, D. Sarkar and K. Pardesi, Anticancer potential of AgNPs synthesized using Acinetobacter sp. and Curcuma aromatica against HeLa cell lines: A comparative study, *J. Trace Elem. Med. Biol.*, 2020, **62**, 126630.
69 B. Pem, I. M. Pongrac, L. Ulm, I. Pavičić, V. Vrček, D. D. Jurašin, M. Ljubojević, A. Krivohlavek and I. V. Vrček, Toxicity and safety study of silver and gold nanoparticles functionalized with cysteine and glutathione, *Beilstein J. Nanotechnol.*, 2019, **10**, 1802–1817.

